中國機械工程學刊第四十五卷第三期第 279~292 頁(民國一百一十三年)
Journal of the Chinese Society of Mechanical Engineers, Vol.45, No.3, pp279~292 (2024)

Research On the Fault Detection Method of Centrifugal Pump Rotor Misaligned

Yechun Li*, Lingfeng Tang* and Weiwei Duan**

Keywords： centrifugal pump; rotor misalignment; fault diagnosis; SVM support vector machine

ABSTRACT

Aimed at the problems of low detection accuracy and poor adaptability of centrifugal pump rotor misalignment fault, the mechanism and characteristics of centrifugal pump rotor misalignment fault were discussed. The overall scheme design of the centrifugal pump rotor misalignment fault diagnosis was completed. The vibration state of rotor stability and misalignment fault was simulated, and the time domain curve, order spectrum, and axis trajectory diagram under different states were obtained. A frequency band division method based on improved empirical wavelet and scale-space theory, and a centrifugal pump rotor misalignment fault diagnosis and identification method based on SVM support vector machine optimized by the genetic algorithm are proposed. A centrifugal pump rotor vibration simulation test bench was built to simulate the centrifugal pump rotor misalignment fault. The proposed fault diagnosis method was used for fault identification. The experimental results show that the recognition accuracy of the method was 93 %, which can effectively diagnose faults and optimize fault identification. The feasibility and superiority of the method for centrifugal pump rotor misalignment fault identification were verified, and the research on the centrifugal pump rotor misalignment fault detection method was completed.

INTRODUCTION

Centrifugal pumps are a piece of common mechanical equipment in all kinds of projects, widely used in industrial mining, agricultural production, transportation, and other fields, accounting for 70% of the total number of pump products. In actual production applications, the rotor failure of centrifugal pumps has become a difficult problem for relevant researchers at home and abroad0 To determine whether a centrifugal pump is malfunctioning or not, it mainly relies on the abnormal noise and vibration during the operation of the centrifugal pump, and the current diagnosis methods for rotor misalignment faults are mainly based on mathematical models, signal processing, and knowledge while combining different artificial intelligence algorithm methods.

Stopa M M et al.(2011) used a method based on the spectral analysis of load torque signal to diagnose the early failure of centrifugal pump cavitation with good results. V Muralidharan; V Sugumaran0 (2013) A vibration-based fault diagnosis method was investigated for a single-stage centrifugal pump with the comprehensive simulation of normal, cavitation, impeller, and other faults, and different wavelets were classified using the fuzzy logic algorithm (99.84%). Using discrete wavelets to extract features, rough set theory, and classification algorithms are promising for single-stage centrifugal pump fault diagnosis.S Alabied et al. (2019) studied the classification of centrifugal pump faults based on current signals and applied it to the diagnosis of motor current signals by using the statistical characteristics of motor current signals. The results show that ITD is effective in extracting the characteristics of the largest amount of information in motor current signals. The SVM diagnosis method based on ITD classifies the simulated faults of centrifugal pumps, which has higher classification accuracy than that of SVM directly applied to the original data, and has better application value. Yu Chen; Hongmei Liu (2018) proposed a centrifugal pump fault diagnosis method based on SWT and SVM to select the vibration signal of the motor-driven centrifugal pump. The fault forms of centrifugal pumps include bearing roller fault, bearing inner ring wear, bearing outer ring wear, and centrifugal pump impeller wear. The fault signal of a centrifugal pump is analyzed by wavelet transform time-frequency analysis, and the frequency domain characteristics of the centrifugal pump fault signal are extracted and classified by a support vector machine,

Paper Received September, 2023. Revised January, 2024. Accepted February, 2024. Author for Correspondence: Yechun Li

**Yechun Li Student, School of Mechanical Engineering, Anhui Polytechnic University, Wuhu, Anhui 241000, China.*

**Lingfeng Tang Professor, School of Mechanical Engineering, Anhui Polytechnic University, Wuhu, Anhui 241000, China.*

***Weiwei Duan Student, School of Mechanical Engineering, Anhui Polytechnic University, Wuhu, Anhui 241000, China.*

to realize the fault diagnosis of the centrifugal pump. M S Kovalchuk et al. (2018) studied the current diagnostic methods of ESP and examined the problems of its diagnosis and identified the main standard faults of ESP, mechanical faults such as bearing wear, bushings, and guide lobe hubs, shaft misalignment, shaft unbalance, etc., causing stator base or top seat faults, leading to rotor eccentricity, ladle compression force weakening, electromagnetic faults such as stator winding disconnection or short circuit, leading to changes in consumption current, etc. Ahmad Zahoor et al. (2021) established a new framework for centrifugal pump fault diagnosis by choosing Walsh transform and cosine linear discriminant analysis of fault characteristic coefficients, and the classification results obtained by this method are better than the existing advanced methods in terms of fault classification accuracy. Maamar Ali Saud ALTobi et al. (2019) investigated the classification of centrifugal pump fault states by backpropagation (MLP-BP) trained multilayer feedforward perceptron neural network and genetic algorithm (GA) hybrid trained multilayer feedforward perceptron neural network (MLP-GABP), support vector machine (SVM) classifier, and the results showed that MLP-BP showed better performance than MLP-GABP and SVM using less number of features performance, and SVM performs better when using polynomial kernel functions using fewer features and parameters. Zhu Yu and Xiong Xiaohu0 et al. (2016) used the German VIBXPERT-II vibration detection analyzer to perform experimental measurements and data analysis on the axial and radial vibration of centrifugal pump units under normal and different fault conditions, and obtained time domain and spectral plots for normal and fault conditions to verify the effectiveness of the vibration-based analysis method.

The present study designs a general scheme for centrifugal pump rotor misalignment fault diagnosis, builds a simulation experimental platform for centrifugal pump rotor fault diagnosis, collects the actual vibration data of centrifugal pump rotor fault according to the simulated centrifugal pump rotor misalignment fault, and proposes a fault diagnosis identification vibration method with an improved empirical wavelet and genetic optimization of SVM based on the collected fault vibration signal, and provides data based on this theoretical analysis. Through experiments, it is concluded that the method can effectively diagnose faults as well as optimize fault identification, thus verifying the feasibility and effectiveness of the centrifugal pump rotor fault diagnosis method proposed in this paper.

ANALYSIS OF FAULT FAILURE OF CENTRIFUGAL PUMP

The rotor is the main component of centrifugal pumps, understanding and mastering its common failure rotor misalignment fault classification and mechanism, can optimize the operating conditions of centrifugal pumps and improve the accuracy of its fault identification.

Rotor structure of the single-stage single-suction plastic centrifugal pump

The rotor includes the impeller, bearing, pump shaft and sleeve, and other parts, as shown in Figure 1. During operation, the impeller and rotor of centrifugal pumps can cause centrifugal inertia force or moment of inertia in the rotor center of mass due to structure, assembly, non-working operation, etc., which makes the equipment vibrate and reduces the working accuracy and reliability of the equipment. To effectively solve this problem, it is especially important to study the misalignment of impellers and rotors0

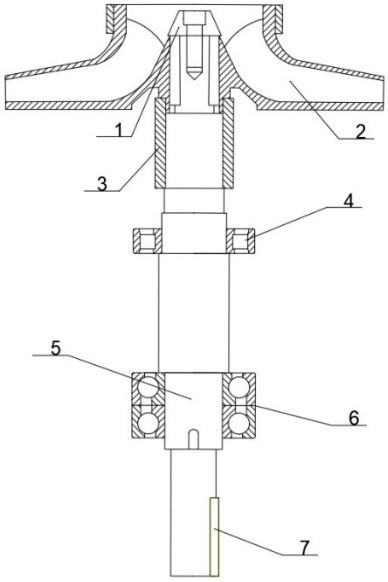

1-Back cap 2-Impeller 3-Sleeve 4-Support bearing
5 - Pump shaft 6 - Axial bearing 7 - Key
Fig. 1.Rotor diagram

Centrifugal pump rotor misalignment fault classification and fault vibration analysis

Fault classification of centrifugal pumps with rotor misalignment due to structure, assembly, non-working operation, etc. includes:

1) In the case of parallel misalignment, the shaft system has an exciting force related to the double frequency of the rotational speed change.

2) Angle misalignment means that the shaft system has two times the frequency excitation force with the change of rotational speed. Angle misalignment and rotational speed will affect the frequency excitation force.

3) Bearing misalignment results in misaligned excitation forces, fluid non-constant forces, and

gravitational forces.

The specific vibration characteristics of the centrifugal pump rotor misalignment fault are as follows.

1) Features of the characteristic spectrum in angular misalignment:

When the angle is misalignment, the fundamental frequency and the double frequency spectrum are generated and the axial vibration occurs ;

The triple frequency generated when the angle is misalignment is more than 30 ~ 50 % ;

The phase difference of axial vibration is 180 ° when the angle is misalignment.

2) Characteristics of the parallel misalignment feature spectrum:

The radial vibration generated when parallel misalignment is relatively large ;

The frequency spectrum at this time : the second harmonic frequency is relatively large, often exceeding the fundamental frequency, and in severe cases, more harmonic high-order vibrations will be generated ;

The phase difference of axial vibration caused by parallel misalignment is 180 °.

3) Bearing misalignment fault characteristics:

When the bearing misalignment is too large, additional force and torque are generated on the centrifugal pump rotor.

At this time, the spectrum is the fundamental frequency and the double frequency ;

The vibration caused by bearing misalignment is mainly axial vibration.

This misalignment is generally eliminated by disassembling and reinstalling the bearing.

RESEARCH ON THE OVERALL SCHEME DESIGN OF CENTRIFUGAL PUMP ROTOR MISALIGNMENT FAULT DIAGNOSIS

To better analyze the centrifugal pump rotor misalignment fault, vibration analysis is used for diagnosis. The vibration information of rotating machinery faults is not only simple and reliable in signal acquisition, data processing, and fault identification, but also has good sensitivity to different faults.

Fault diagnosis method of centrifugal pump rotor misalignment

According to the fault mechanism of the centrifugal pump, the processed vibration signal is transformed into valid information that can identify and reflect the operation of the centrifugal pump. Then, according to the mastered fault information and state parameters to classify them, to further ensure the normal use of the centrifugal pump, to achieve the fault diagnosis of the centrifugal pump, the data is processed by the computer and saved into .mat data format. The speed governor, sensor, motor, vibration meter, plotter, and computer are connected to a test system, as shown in Fig. 2.

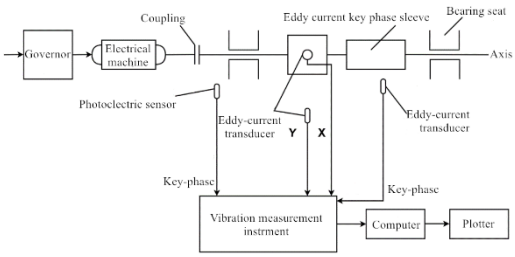

Fig. 2 Overall scheme schematic

Overall scheme experimental device

In this paper, we design and build an experimental device to simulate the vibration of a centrifugal pump, which can reproduce various vibration phenomena generated by rotating machinery. It consists of a motor mounting board, photoelectric sensor, eddy current sensor, ZD-220T DC motor, etc., as shown in Fig. 3.

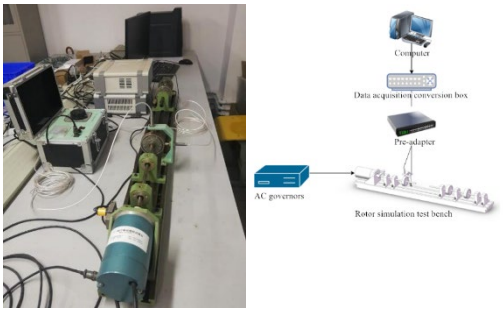

(a) (b)

Fig. 3 Centrifugal pump simulation experiments (a) centrifugal pump experimental bench setup; (b) experimental simulation flow chart

Install the experimental platform as shown in Fig. 3 and connect the sensor with the measuring instrument. The x- and y-direction eddy current sensor is installed on the sensor bracket, and the clearance between the probe end face and the outer circle of the rotor is adjusted according to the median value of the linear range of the sensor; the photoelectric sensor is installed at the reflective mark directly opposite to the coupling. In the case the check is correct, you can turn on the power, and start the test bench. According to the requirements of turning the button of the governor gradually increase the rotor speed, and through the computer in the rotating machinery vibration state monitoring and analysis system to observe the vibration situation.

Centrifugal pump rotor fault simulation experiment steps and fault display

The simulation experiments of the rotor under misalignment (the pad height is close to one end of the coupling bearing) and normal state are set respectively. The rotor of the centrifugal pump in different states will also be displayed differently in the rotating machinery vibration state monitoring and analysis system.

The time domain curve of the displacement signal in the misalignment state is shown in Fig..4.At this time, the peak and trough of the curve are quite different.

1、In the order spectrum, the characteristic frequency is 2 times the frequency, often accompanied by 1 times the frequency and 3 times the frequency, as shown in Fig. 5.

2、In the axis orbit diagram, the axis orbit curve is ' 8 ' shaped, not elliptical, indicating that the axis does not maintain balance, and there is a certain misalignment phenomenon, such as Fig. 6.

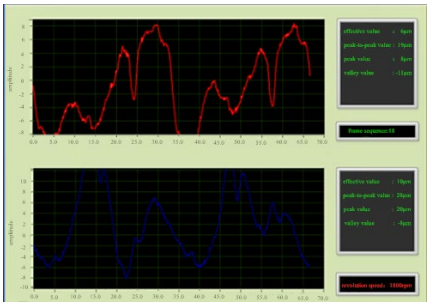

Fig. 4 Misalignment time domain curve

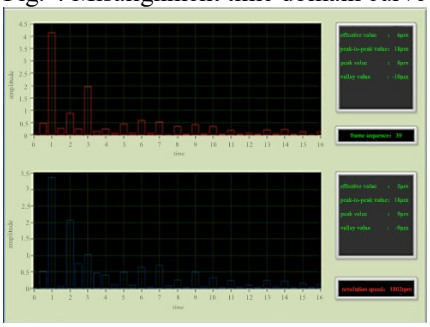

Fig. 5 Misalignment order spectrum characteristic frequency plot

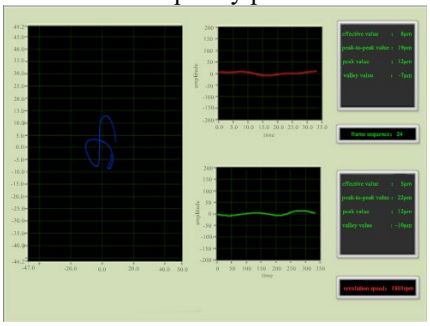

Fig. 6 Misalignment axis trajectory diagram

Under normal conditions, the time domain curve of the displacement signal is shown in Fig. 7. At this time, the fluctuation amplitude of the curve is relatively small, and the peak is relatively flat when it drops.

1、In the order spectrum, it is generally the fundamental frequency and close to the sine wave, as shown in Fig. 8.

2、In the axis orbit diagram, the axis orbit curve is elliptical, indicating that the axis is relatively balanced at this time, and there is no misalignment phenomenon, as shown in Fig. 9.

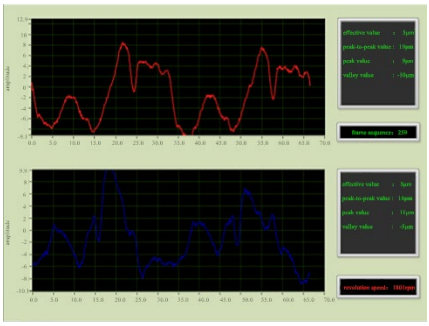

Fig. 7 Normal signal time domain curve

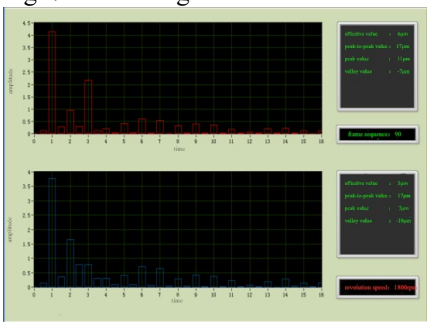

Fig. 8 Normal signal order spectrum characteristic frequency diagram

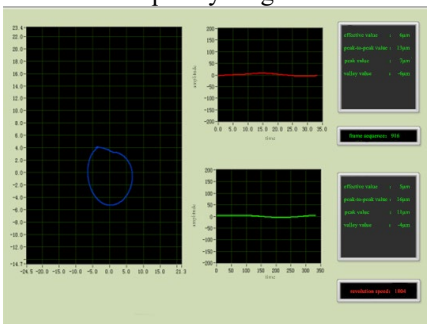

Fig. 9 Normal signal axial trajectory diagram

ANALYSIS OF ROTOR MISALIGNMENT FAULT DIAGNOSIS BASED ON IMPROVED EMPIRICAL WAVELET CENTRIFUGAL PUMP

Fault vibration signals of centrifugal pump rotor misalignment are nonlinear and non-stationary signals. The joint time-frequency domain analysis method is commonly used to feature the extraction of centrifugal

pump rotor fault vibration signals. The EWT method, one of the more popular methods in recent years, has achieved some results in the field of signal processing. This section will focus on the principles of the EWT method and investigate further improvements to it.

The basic principle of empirical wavelet and its frequency band division method

The EWT method divides the Fourier spectrum of a signal, constructs a wavelet filter bank on the continuous interval and filters it, and obtains a set of empirical mode components by signal reconstruction. This method adaptively identifies and extracts feature information in the Fourier spectrum of a signal using a wavelet filter bank with tight support characteristics.

Fourier Schematic diagram of axis segmentation As in Fig. 10. the Fourier spectrum is divided into N bands and $N+1$ boundary points are found. Calculating all the maximum value points in the Fourier spectrum (M points,0 and π excluded) and arranging them in descending order, the following two scenarios can occur:

$M > N$, take the first $N-1$ maximum point as the boundary point;

$M < N$, reset parameter N so that $N = M$.

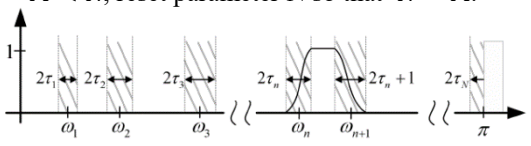

Fig. 10 Segmentation of Fourier axis

Let $f(x) \in [0,\pi]$ be a Fourier spectrum, and define the kernel function $g(n;t) = \frac{1}{\sqrt{2\pi nt}} e^{-x^2/(2t)}$, t is the scale parameter, which is the theory of scale space, this paper takes t = 0.5, the collected centrifugal pump rotor fault vibration signal continuous scale space discretized as in Equation 1.

$$L(m,t) = \sum_{i=-M}^{+M} f(m-n)g(n;t) \quad (1)$$

The kernel function and the scale parameter are discretized, such as Equation 2 :

$$g(n;t) = \frac{1}{\sqrt{2\pi t}} e^{-N^2/(2t)} \quad (2)$$

The kernel function is a vector of length 7, where $M = C\sqrt{t}+1$, and $3 \le C \le 6$. In general, when $C = 6$ When the error is less than 10^{-9}, this paper takes $C = 3$.

$$\sqrt{t} = s\sqrt{t_0} \quad (3)$$

In Equation 3, the

$S = 1,\cdots, S_{max}$, and S_{max} are integers, in general, and $\sqrt{t_0} = 0.5$, the $S_{max} = 2x_{max}$.

Substitution of Equation 3 gives the discrete scale-space $L(x,t)$ as in Equation 4 and Equation 5.

$$L(x,t) = \sum_{n=-M}^{+M} f(x-n)g(n;t) \quad (4)$$

$$g(n;t) = \frac{1}{\sqrt{2\pi s^2 t_0}} e^{-N^2/(2s^2 t_0)} \quad (5)$$

After discretization, the $L(x,t)$ can be considered as a function of the number of minimal values of the variable x. If the initial number is N_0, then the scale space curve is $C_i (i \in [1, N_0])$ and the length is L_i.

In the band division method of scale space theory, all minimal value points in the space correspond to a curve. Selecting a suitable threshold value T0 Using the Otsu algorithm (Otsu), T = 159 was obtained.

A Gaussian kernel function is set, the spectrum is smoothed with the Gaussian kernel function, the band boundary points obtained at that time are recorded, and the number of minima for each frequency point at each scale is calculated. The scales and band boundaries form a two-dimensional scale space, and a threshold is generated using a method such as maximum interclass difference T. By comparing the relationship between the curve length and the threshold T, the desired frequency band cut-off point is selected. The above smoothing process is repeated continuously, and the band demarcation points that do not meet the conditions are gradually filtered out, leaving the desired demarcation points.

Improvement principle of empirical wavelet transform and comparative analysis

The classical scale space method selects too many band demarcation points, which will cause the band-breaking phenomenon and affect the analysis. An improved empirical wavelet transform band division method is proposed to adopt the band energy to select the band demarcation points, which makes the divided bands more reasonable and practical. The steps of the method are shown in Fig. 11.

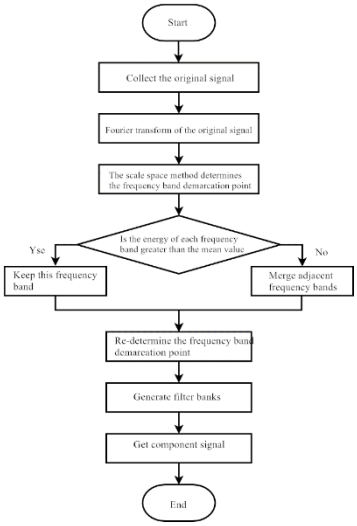

Fig. 11 Flow chart of empirical wavelet dividing a frequency band

Fig. 11 shows that after the classical scale space method is used to find out the dividing point of the primary frequency band of the centrifugal pump rotor fault signal, the energy of each frequency band of the centrifugal pump rotor fault signal is calculated and the average energy value is obtained. Since the energy of the main frequency of the centrifugal pump rotor fault signal must be greater than the average energy, the centrifugal pump rotor fault signal band with energy greater than the average energy is retained, and the two adjacent centrifugal pump rotor fault signal bands with energy lower than the average energy are combined. If there are multiple adjacent centrifugal pump rotor fault signal bands below the average energy, these bands can be combined at once. After such processing, the final centrifugal pump rotor fault signal frequency band cut-off point is significantly smaller than the initial result, effectively avoiding the problem of centrifugal pump rotor fault signal frequency band breakup.

Improved comparative analysis:

Establish the expression for the multi-harmonic signal of a centrifugal pump rotor:

$$x(t) = 0.6\sin(2\pi f_1 t) + \sin(2\pi f_2 t) + 1.5\sin(2\pi f_3 t) + 0.8\sin(2\pi f_4 t) + noise \quad (6)$$

In Equation 6, $f_1 = 900, f_2 = 2500, f_3 = 400, f_4 = 1200$ are harmonic frequencies. The sampling frequency is 10340 Hz, and the time domain diagram is shown in Fig. 12. It is difficult to extract fault information from the time domain diagram. The spectrum is shown in Fig. 13.

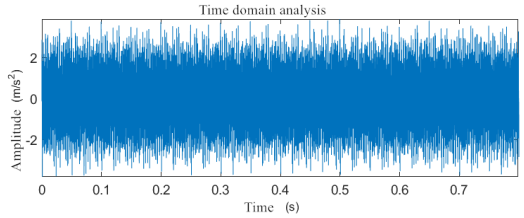

Fig. 12 Time domain diagram of the signal

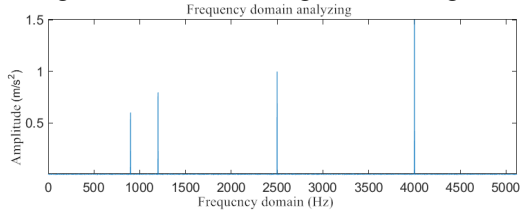

Fig. 13 Frequency spectrum of the signal

The scale space curve of the multi-harmonic signal of the centrifugal pump rotor is plotted in Fig. 14. The threshold value is indicated by the red line in the figure, and the scale space curve of the initial very small value point is indicated by the blue line.

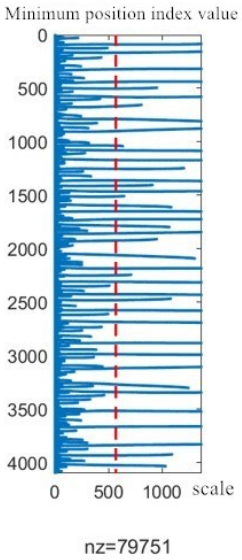

Fig. 14 Scale Space Curve Chart

The initial band division of the multi-harmonic signal of the centrifugal pump rotor obtained by the classical scale-space method is shown in Fig. 15. The band division is performed by using the improved energy-based spatial scale method, as shown in Fig. 16.

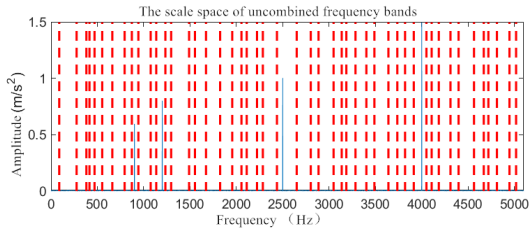

Fig. 15 Initial band division

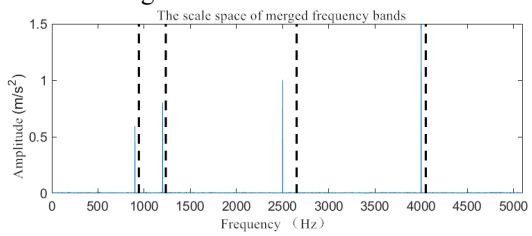

Fig. 16 Improved band division

Comparing Fig. 15 and Fig. 16, it can be concluded that the number of bands obtained by the classical spatial scale-based method and the improved energy-based spatial scale method are 41 and 5, respectively. the number of bands of the centrifugal pump rotor multi-harmonic signal is greatly reduced and the problem of band breaking of the centrifugal pump rotor multi-harmonic signal is effectively improved. The filter set is constructed, and Fig. 17 shows the multi-harmonic signal components of the centrifugal pump rotor obtained after filtering.

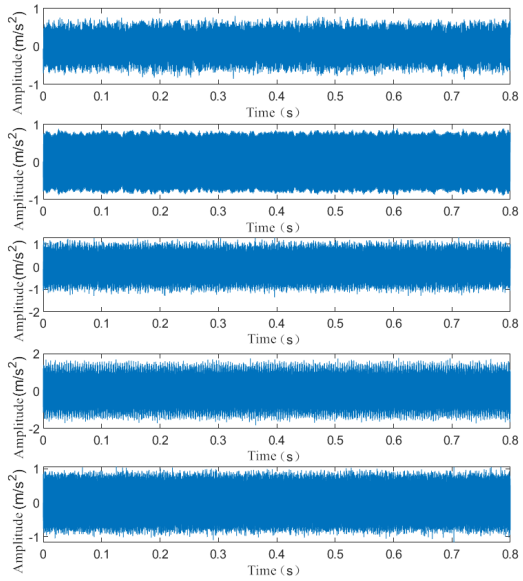

Fig. 17 Component signal obtained after filtering

Fig. 18 shows the spectrum of the centrifugal pump rotor multi-harmonic signal component signal after improved empirical wavelet transform processing. The frequencies 0～1KHz are given for observation since the high-frequency components of the centrifugal pump rotor multi-harmonic signal are placed in the low-frequency band during modulation, while the frequencies of the centrifugal pump rotor multi-harmonic signal are included. It can be concluded that after the improved energy scale space-based method of preferentially selecting the frequency band of centrifugal pump rotor multi-harmonic signal, the fault characteristic frequencies and their 2-fold and 3-fold frequencies are more obvious and the fault type can be easily determined.

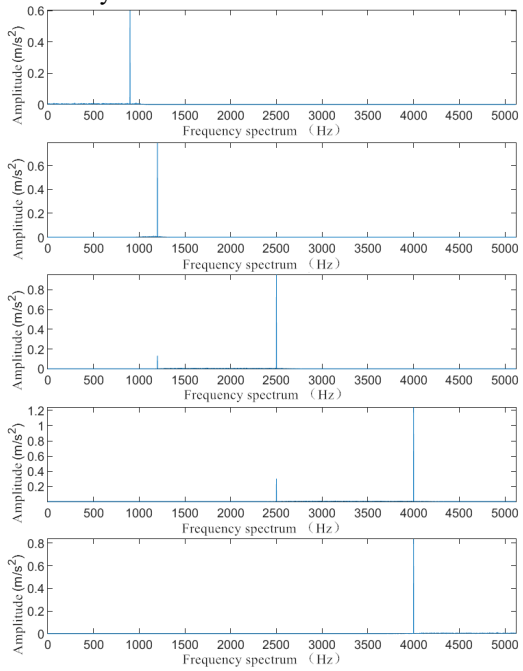

Fig. 18 Spectrum of component signals after improved empirical wavelet transform processing

From the signal spectrum Fig. 13 and Fig. 18, it can be seen that the generation of fundamental, 2-fold, and 3-fold frequencies of the improved method is significantly better than that of the classical scale-space method, and the 4-fold frequency can be observed. It can be concluded that the improved method of secondary screening based on the initial frequency band dividing points of energy proposed in this paper is effective, and the number of frequency band dividing points of a multi-harmonic signal of centrifugal pump rotor is reduced by this method, and the problem of multi-harmonic signal band breaking of centrifugal pump rotor is improved and computation is reduced.

Optimizing Support Vector Machines

Principles of Support Vector Machines have better learning, generalization, and small sample classification capabilities than traditional artificial neural networks.

With a training set$(a_i,\ b_i)$,$i = 1,2,L,Q$, Q: the number of samples, in this paper, there are 900 samples, 3 types, 300 of each type. $a_i \in F_n$, and a_i: the input data, the F_n: sample space. $b_i = \{-1,\ +1\}$, and b_i: the output category. Let the original space F_n of 2 vectors: α and β. By the theory of generalized functions, define the kernel function $k(\alpha,\ \beta) = \Phi(\alpha)\Phi(\beta)$, and Φ: the original space is mapped to a higher dimensional space. Unknown samples a_j Decision model:

$$f(a_j) = sgn(\ )[\sum_{i=1}^{n} \delta_i b_i k(a_i, a_j) + h'] \quad (7)$$

where

δ_i--lagrange multipliers;

h'--bias amount;

sgn( )--symbolic function.

The radial kernel function was selected by comparison as the kernel function of SVM, as in Equation 8:

$$K(x_i, x) = exp\left\{-\frac{\|x_i - x\|}{-2\sigma^2}\right\} \quad (8)$$

Genetic algorithm for optimization of support vector machines.

Using Genetic Algorithm Optimization parameters, the maximum number of evolutionary generations: 500, maximum number of populations: 50,c range of variation: (0,100],g range of variation: [0,1000], cross-validation parameters: 5. Initial parameters evolutionary generations: 1, number of populations; 20, number of iterations; 200. root mean square error (MSE) of fitness function values:

$$fit_{MSE} = \sqrt{\frac{\sum_{i=1}^{n}(y_i - f_i)^2}{n}} \quad (9)$$

where

fit--Adaptation function;

y_i--sample truth values;

f_i--predicted values;
n--Sample size.

A genetic algorithm (GA) was used to determine the optimal parameters of the SVM model, and the process is shown in Fig. 19.

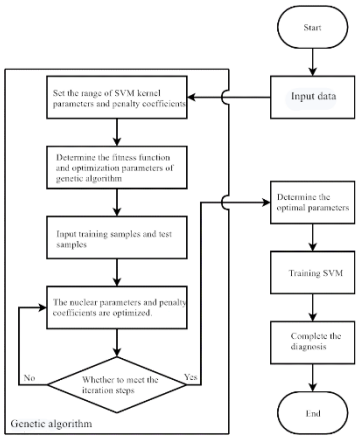

Fig. 19 Flow chart of SVM for genetic algorithm optimization

The processed data are input into the support vector machine, and the SVM kernel function and penalty coefficient range are set i.e., the kernel function c varies in the range: (0,100] and the penalty coefficient g varies in the range: [0,1000]. The root mean square error is used as the fitness function value, and the kurtosis value and the scattering entropy are used as the merit-seeking parameters. Input training samples and test samples, optimize the kernel function and penalty coefficient, determine whether they satisfy the iteration step number 200, continue to optimize the kernel function and penalty coefficient if they do not satisfy, satisfy the iteration step number 200, determine the optimal parameters to get the optimal kernel function g=0.081 and the optimal penalty factor c=77.7667, train the SVM, and complete the diagnosis.

For the centrifugal pump, rotor misalignment fault vibration signal characteristics, the improved EWT, and genetically optimized support vector machine are used for fault diagnosis, and the diagnosis steps are as follows:

1) Selection of the study object: vibration signal data of faulty and non-faulty centrifugal pumps.

2) Decompose the noise-reduced signal using the improved EWT method to obtain multiple IMF components.

3) Calculate each IMF cliff value and scattering entropy to construct the key feature vector.

4) Selected partial fault and normal state feature vectors by genetic optimization for SVM machine learning.

5) The remaining feature vectors are fed into the genetically optimized SVM fault identification.

EXPERIMENTAL BENCH

CONSTRUCTION AND DATA PROCESSING

This chapter will further elaborate on the vibration signal of the centrifugal pump rotor misalignment fault collected by using simulation experiments.

Simulation bench construction

A simulation bench is built to collect the vibration signals of the centrifugal pump rotor in misaligned and normal conditions and to extract the features and identify the faults. The components of the simulation bench are described below.

The experimental platform mainly consists of bearing housing, base, motor mounting plate, drive shaft, eddy current / photoelectric sensor, coupling, ZD-220T DC motor drive supply power, and step-less adjustment. Centrifugal pump simulation experimental platform design and physical diagram, as shown in Fig. 20, are the main technical parameters of the test bench as shown in Table 1.

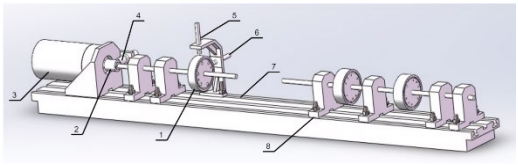

(a)

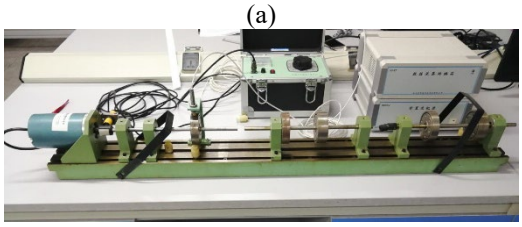

(b)

Fig. 20 Experimental platform design and physical diagram
(a) Experimental table design drawing
(b) Physical drawing of the experiment table
1-Rotor 2-Coupling 3-Motor 4-Optical sensor 5-Vertical eddy current sensor
6-Horizontal eddy current sensor 7-Base 8-Bearing housing

Table 1 Main technical parameters of the test bench

Part Name	Parameter Name	Parameter Value
Rotors	Size	Φ76*25mm and Φ76*19mm
	Quality	800g and 600g
Revolution axis	Diameter	9.5 mm
	Maximum deflection	No more than 0.03mm
Base	Length*width*height	1200mm*108mm *135mm
	Quality	About 45kg

Centrifugal pump condition experiment

Two states, two directions, 300 data samples in each direction, 2048 data points per sample, 614,400 in total, 600 sets in total, 810 training sets, and 60 test sets, at a speed of 1800 r/min. From this failure,90% is randomly selected as the training sample and the rest as the test sample.

(1) rotor normal state experiment

To facilitate the observation of the graph, 324 sampling points are taken in the screenshot of the time-frequency plot, and 8192 sampling points are taken in all other plots. Fig. 21 shows the time domain signal graph of the normal state.

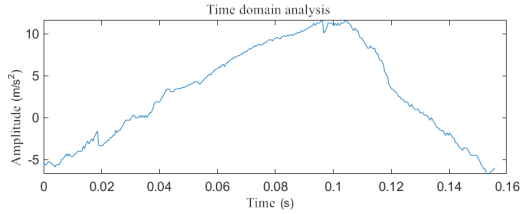

(a)

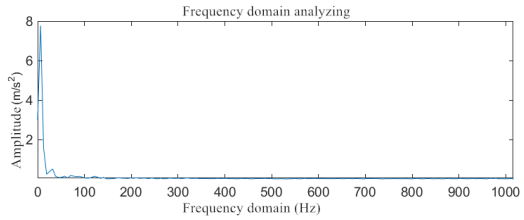

(b)

Fig. 21 Time and frequency diagram of the centrifugal pump rotor experimental data in normal condition
(a) Time domain diagram; (b) Frequency domain diagram

It can be seen from Fig. 21 that the frequency component of the centrifugal pump rotor experimental data in the normal state is relatively simple, and the time domain waveform in the normal state is very close to the sine waveform, excluding other influencing factors in the experiment.

(2) rotor misalignment experiment

The rotor misalignment was simulated by padding the bearing end of the coupling as shown in Fig. 22. 1800 r/min speed, the rotor misalignment time, and the frequency diagram is shown in Fig. 23. There are 2 times frequency peaks in the time domain diagram, and 1 frequency doubling, 2 frequency doubling, or even 3 frequency doubling in the spectrum diagram.

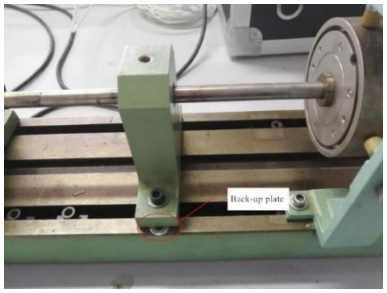

Fig. 22 Rotor misalignment experimental setup

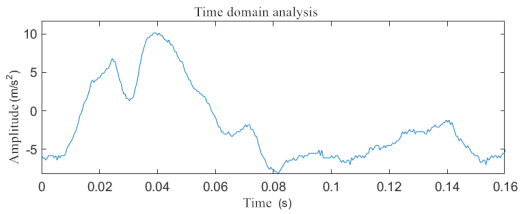

(a)

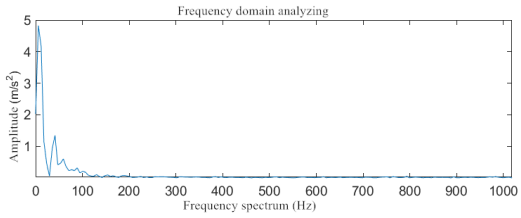

(b)

Fig. 23 Time and frequency diagram of centrifugal pump rotor experimental data in the misaligned condition
(a) Time domain diagram; (b) Frequency domain diagram

(3) test bench centrifugal pump design and manufacture

A single-stage, single-suction plastic centrifugal pump is used as the experimental object, as shown in Fig. 24.

Fig. 24 Single-stage single-suction plastic centrifugal pump

The parameters of a plastic centrifugal pump are designed and calculated, and the parameters of a plastic clear water type centrifugal pump are shown in Table 2 Device cavitation margin NPSHa (m): 4;

Table 2 Plastic clear water type centrifugal pump parameters

Parameters	Flow rate Q (m^3/h)	Head H (m)	Rotational speed n (r/min)
Numerical value	50	10	1450

The structural parameters of the centrifugal pump were obtained after the design as shown in Table 3.

Table 3 Plastic centrifugal pump design parameters

Performance Parameters		Geometric dimensions	
Flow rate Q(m^3 /h)	50	Impeller inlet diameter (mm)	50
Head H(m)	10	Impeller outlet diameter(mm)	60
Rotational speed n(r/min)	1450	Blade inlet width(mm)	11
Specific speed n_s	185.9	Blade outlet width(mm)	10
Width of worm shell(mm)	20	Blade inlet mounting angle (°)	18
Diameter of worm shell base circle(mm)	83	Blade outlet installation angle (°)	32
Number of blades (pcs)	6	Wrap angle φ (°)	120

Experimental data acquisition

The restoration fault diagnosis process utilizes the ZT-3 rotor vibration simulation test bench to collect signals from rotor misalignment and normal states. The experimental measurement points are arranged as shown in Fig. 25. The speed range of the collected data is 1200 to 2500 rpm, and the main study speed is 1800 rpm. Each state collects 300 samples from both vertical and horizontal directions, and 2048 data points for each sample, that is, a total of 614400 points are collected in each state.

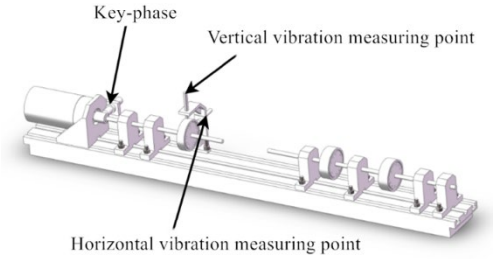

Fig. 25 Rotor measurement point arrangement diagram

Since there are many data collected for each group of experiments, only some of the experimental data collected for the two states of normal and misalignment are given here, see Tables 4 and 5.

Table 4 Normal state experimental data collection

Serial number	Rotational speed (rpm)	Effective value (μm)	Peak-to-peak (μm)	Peak (μm)	Valley value (μm)
1	1801	6.31	17.25	11.95	-7.36
2	1804	5.15	17.89	7.54	-10.19
3	1803	6.73	13.96	7.03	-6.16
4	1801	5.43	16.23	11.69	-4.39
5	1800	5.48	19.77	9.00	-10.49
6	1801	5.27	16.16	11.50	-5.64
7	1804	6.13	16.14	8.67	-9.05
8	1802	6.35	17.96	8.98	-8.98
9	1802	5.84	16.53	8.7	-9.81
10	1803	6.55	18.54	8.28	-9.27

Table 5 Experimental data collected in the non-alignment state

Serial number	Rotational speed (rpm)	Effective value (μm)	Peak-to-peak (μm)	Peak (μm)	Valley value (μm)
1	1803	6.47	19.39	8.98	-11.05
2	1802	10.54	28.80	20.93	-8.01
3	1802	6.67	18.71	8.65	-10.78
4	1804	5.78	18.14	9.22	-9.21
5	1801	8.55	19.84	12.76	-7.01
6	1800	5.62	22.66	12.60	-10.63
7	1803	5.01	19.28	9.71	-10.43
8	1802	5.27	16.23	11.19	-5.15
9	1801	7.63	20.22	10.13	-9.17
10	1804	6.98	19.76	9.83	-11.02

Data Processing and Conclusion

The fault vibration signal of the centrifugal pump rotor is a non-stationary signal. The improved empirical wavelet transform is used to extract useful information from the fault vibration signal of the centrifugal pump rotor. The spectral division of the improved empirical wavelet transform of the signal obtained in two states is shown in Fig. 26 and Fig. 27.

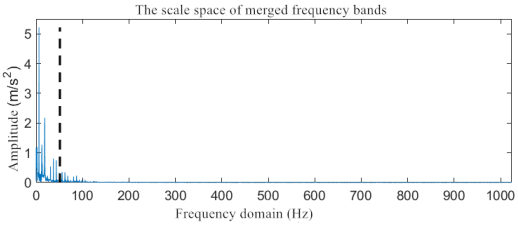

Fig. 26 Spectrum division after normal state improved empirical wavelet transform

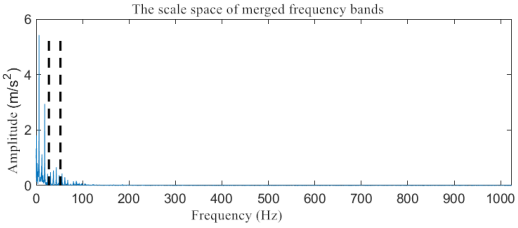

Fig. 27 Spectrum division after improved empirical wavelet transform of the uncentered state

The spectrum of Fourier in two states was divided into 3 bands, 2 bands, and 2 bands respectively after the decomposition of ESEWT, the number of bands was less and the band-breaking phenomenon was improved. The filter banks were constructed and the component signals of three states were obtained as shown in Figs. 28, 29, 30, and 31, respectively.

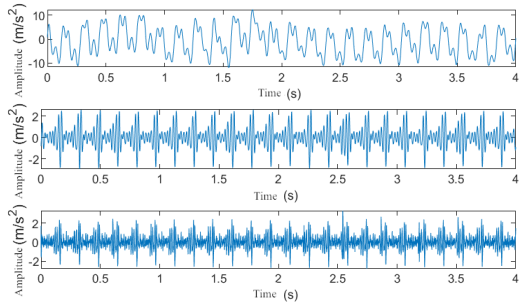

Fig. 28 Component signal plot after improved empirical wavelet transform in misalignment state

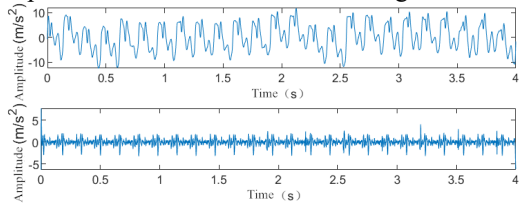

Fig. 29 The component signal after improved empirical wavelet transform in a normal state

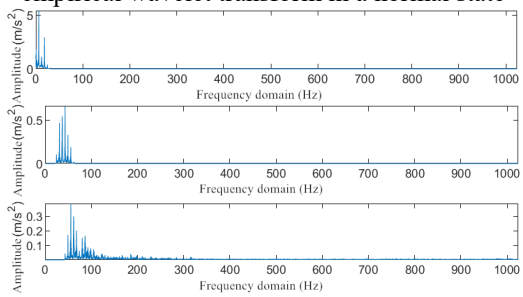

Fig. 30 Spectrum after improved empirical wavelet transform in misalignment state

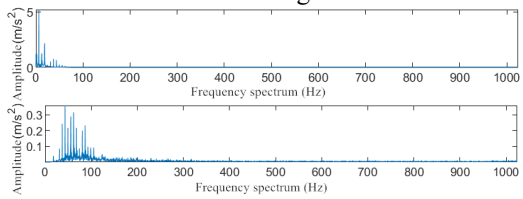

Fig. 31 Spectrum after improved empirical wavelet transform in normal state

ESEWT the fault vibration signal is decomposed into component signals, and the scattering entropy of the component signals and the cliff value of each vibration signal are calculated to form the feature vector. One set of representative calculation results is given, which can distinguish the type of centrifugal pump rotor fault, as shown in Table 6 (the mean value of scattering entropy of component signals and the mean value of stiffness of each vibration signal in different states).

Table 6 Feature vectors

	Normal state	Rotor misalignment
Cliffness	2.9879	3.3988
Dispersion entropy	3.5325	3.6034

The kurtosis and dispersion entropy feature parameters are input into the SVM model and trained in the genetically optimized SVM model. The following is a test experiment of SVM without genetic optimization and SVM after genetic optimization. The total number of samples in the data set is 600, and 40 groups of samples in each category are selected for SVM parameter optimization experiments. Among them, 90 % of the samples are used for training, and 10 % of the samples are used for testing. The kernel function g and penalty factor c of SVM are 0.0797 and 77.7559, respectively. The curve of genetically optimized SVM for finding the best parameters is shown in Fig. 32. It is concluded that the optimal kernel function g and penalty factor c are 0.0801 and 77.7667, respectively.

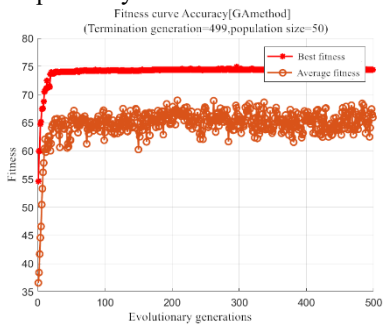

Fig. 32 Adaptation curves of the optimal parameters for genetic search

A conventional SVM was used for fault identification, and the actual results obtained were compared with those obtained by prediction, as shown in Fig. 33. The sample data and test data were then analyzed using the genetically optimized parameters added to the SVM, and the results obtained are shown in Fig. 34.

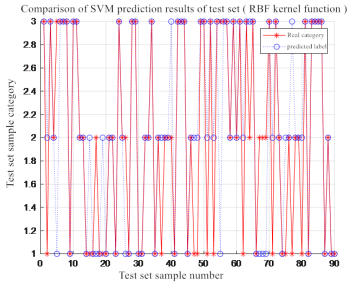

Fig. 33 SVM classification result graph

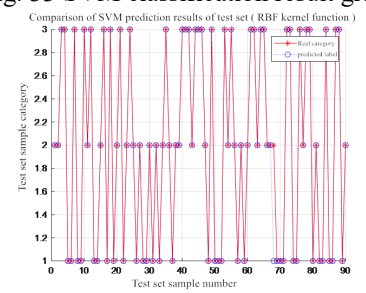

Fig. 34 SVM classification result graph with genetic optimization

The classification results of SVM and genetically optimized SVM for this dataset are shown in Tables 7 and 8 below:

Table 7 SVM sample test identification results

	Correctly classified samples	Misclassification sample	Classification Accuracy
F_1	83	7	78.89%
F_2	84	6	68.89%
F_3	85	5	80.00%
F_4	86	4	77.78%
F_5	82	8	71.11%
F_6	81	9	76.67%
F_7	87	3	71.11%
F_8	80	10	83.33%
F_9	89	1	68.89%
F_{10}	88	2	75.56%
Average	84.5	5.5	75.223%

Table 8 Identification results of SVM sample test with genetic optimization

	Correctly classified samples	Misclassification sample	Classification Accuracy
F_1	83	7	91.11%
F_2	84	6	92.22%
F_3	85	5	93.33%
F_4	86	4	94.33%
F_5	82	8	90%
F_6	81	9	90%
F_7	87	3	95.56%
F_8	80	10	88.89%
F_9	89	1	98.89%
F_{10}	88	2	97.78%
Average	84.5	5.5	93.21%

From Tables 7 and 8, it can be seen that the identification accuracy of the test sample is about SVM 76%, while the identification accuracy of the test sample genetically optimized SVM is better, about 93%, which verifies that the support vector machine fault diagnosis method based on improved empirical wavelets and genetic optimization is correct and effective, and proves the feasibility and superiority of the method in this paper for the identification of centrifugal pump rotor misalignment faults.

CONCLUSION

(1) Introduced the centrifugal pump rotor structure, analyzed the centrifugal pump rotor misalignment fault characteristics, designed a general scheme for fault diagnosis, carried out vibration signal acquisition for the rotor normal state signal and misalignment fault signal, and observed the centrifugal pump rotor vibration in both states from the rotating machinery vibration state monitoring and analysis system in the computer.

(2) The band division method of empirical wavelet and the band division method based on scale space theory is studied, and a band division method based on improved empirical wavelet and scale space theory is proposed to find the cliffs and scattering entropy of each group of IMF components and input each group of feature vectors into the genetically optimized SVM to complete the fault diagnosis, and the band breakage of the improved empirical wavelet transform method is reduced and the signal The quality of reconstruction is improved. The genetically optimized SVM can better distinguish the faults and the diagnosis accuracy meets the practical requirements.

(3) A centrifugal pump rotor vibration simulation test bench consisting of a computer, sensors, data collectors, etc. was built. It is verified that the support vector machine fault diagnosis method based on improved empirical wavelet and genetic optimization can identify the centrifugal pump rotor misalignment fault with an accuracy of 93%, and the proposed method can effectively identify the centrifugal pump rotor misalignment fault.

AUTHOR CONTRIBUTIONS

Yechun Li had made substantial contributions to design, experimental research, data collection and result analysis; Lingfeng Tang made critical changes to important academic content; Weiwei Duan provided some advice and help.

DATA AVAILABILITY

The data used to support the findings of this study are included in the article.

CONFLICTS OF INTEREST

The authors declare that they have no conflicts of interest to report regarding the present study.

REFERENCES

Xingxin Xiao, Liwei Song, Yixun Zhang, et al. Research on centrifugal pump rotor misalignment fault diagnosis method based on CEEMD and SVM[J]. Fluid Machinery,2022,50(07):85-92.

Peng Zhao. Research on vibration fault diagnosis method and system implementation of the centrifugal pump[D]. North China Electric Power University (Beijing),2011.

Soylemezoglu A, Jagannathan S, Saygin C . Mahalanobis-Taguchi System as a Multi-Sensor Based Decision Making Prognostics Tool for Centrifugal Pump Failures[J]. IEEE Transactions on Reliability, 2011, 60(4):864-

878.
Muralidharan V, Sugumaran V . Rough set-based rule learning and fuzzy classification of wavelet features for fault diagnosis of monoblock centrifugal pump[J]. Measurement Journal of the International Measurement Confederation, 2013, 46(9):3057-3063.
Alabied S , Daraz A , Rabeyee K , et al. Motor Current Signal Analysis Based on Machine Learning for Centrifugal Pump Fault Diagnosis[C]// 2019 25th International Conference on Automation and Computing (ICAC). 2019.
Yu C, H Liu. Centrifugal pump fault detection based on SWT and SVM[J]. Vibroengineering PROCEDIA, 2018, 19(3).
M S Kovalchuk and D A Poddubniy. Diagnosis of Electric Submersible Centrifugal Pump[J]. IOP Conference Series: Earth and Environmental Science, 2018, 115(1): 012026-012026.
Ahmad Zahoor et al. A Novel Framework for Centrifugal Pump Fault Diagnosis by Selecting Fault Characteristic Coefficients of Walsh Transform and Cosine Linear Discriminant Analysis[J]. IEEE ACCESS, 2021, 9: 150128-150141.
Maamar Ali Saud ALTobi et al. Fault diagnosis of a centrifugal pump using MLP-GABP and SVM with CWT[J]. Engineering Science and Technology, an International Journal, 2019, 22(3): 854-861.
Yu Zhu, Xiaohu Xiong. Research on the fault diagnosis of ship rotating machinery based on vibration analysis[J]. Jiangsu Ship,2016,33(05):11-14.DOI:10.19646/j.cnki.32-1230.2016.05.003.
Guangrong Ge. Research on impeller and rotor balancing technology of centrifugal pump[J]. General Machinery,2014(09):92-95.
Man Zhen. Analysis of the misalignment dynamics of a two-span rotor system with a membrane disc coupling[D]. University of Chinese Academy of Sciences (Institute of Engineering Thermophysics, Chinese Academy of Sciences),2019.
Kumar Rajeev et al. A State-of-the-Art Review on the Misalignment, Failure Modes and Its Detection Methods for Bearings[J]. MAPAN, 2022, 38(1) : 265-274.
Guodong Hou. Diagnosis of common faults in the operation of centrifugal pumps [J]. Urban Construction Theory Research: Electronic Edition, 2012, 000(009):1-3.
Ahmad Sajjad and Ahmad Zahoor and Kim JongMyon. A Centrifugal Pump Fault Diagnosis Framework Based on Supervised Contrastive Learning[J]. Sensors, 2022, 22(17): 6448-6448.
Zhu Liu. Fault diagnosis method of the reciprocating compressor based on MRSSD and CMSDE[D]. Northeastern Petroleum University, 2020. DOI:10.26995/d.cnki. disc.2020.000675.
Gilles J, Tran G, Osher S . 2D Empirical Transforms. wavelets, Ridgelets, and Curvelets Revisited[J]. Siam Journal on Imaging Sciences, 2014, 7(1):157--186.
Xingzhou Du. Research on fault diagnosis of rotating machinery based on vibration signal processing and SVM [D]. Harbin Institute of Technology, 2019. DOI:10.27061/d.cnki.ghgdu.2019.005457.
Yunqi Li. Research on the application of empirical wavelet transforms and support vector machines in rolling bearing fault diagnosis[D]. Southwest Jiaotong University,2018.
Parveen P, Thuraisingham B . Face Recognition Using Multiple Classifiers[C]// IEEE International Conference on Tools with Artificial Intelligence. IEEE, 2006.
YZ Wang, ZG Fu, BH Liu, PK Wang. Soft measurement of flue gas oxygen content based on GA-SVM[J]. Chemical Automation and Instrumentation,2017,44(10):937-939.

NOMENCLATURE

δ_i--lagrange multipliers;
h'--bias amount;
sgn( )--symbolic function.
fit--Adaptation function;
y_i--sample truth values;
f_i--predicted values;
n--Sample size.

離心泵轉子不對中故障檢測方法研究

李葉春 唐鈴鳳 段維維
安徽工程大學機械工程學院

摘要

摘要：針對離心泵轉子不對中故障檢測精度低、適配性差等問題，論述了離心泵轉子不對中故障機理及特點，完成了離心泵轉子不對中故障診斷總體方案設計，模擬了轉子穩定和不對中故障下的振動狀態，得到了不同狀態下的時域曲線圖、階次譜圖中和軸心軌跡圖。提出了一種基於改進經驗小波和尺度空間理論的頻帶劃分方法，以及基於遺傳優化的 SVM 支援向量機的離心泵轉子不對中故障診斷

識別方法，搭建了離心泵轉子振動模擬試驗台，模擬了離心泵轉子不對中故障，利用所提出的故障診斷方法進行故障識別，通過實驗得出該方法識別準確率達 93%，能夠有效地診斷故障以及優化故障識別，驗證了該方法對離心泵轉子不對中故障識別的可行性與優越性，完成了離心泵轉子不對中故障檢測方法的研究。